Integration of Bayesian regulation back-propagation neural network and particle swarm optimization for enhancing sub-pixel mapping of flood inundation in river basins

Linyi Li [a]*, Yun Chen [b], Tingbao Xu [c], Chang Huang [d], Rui Liu [b, e], and Kaifang Shi [b, e]

[a] *School of Remote Sensing and Information Engineering, Wuhan University, 129 Luoyu Road, Wuhan 430079, PR China*
[b] *CSIRO Land and Water Flagship, Clunies Ross Street, Canberra 2601, Australia*
[c] *Fenner School of Environment and Society, The Australian National University, Linnaeus Way, Canberra 2601, Australia*
[d] *College of Urban and Environmental Sciences, Northwest University, 1 Xuefu Road, Xi'an 710127, PR China*
[e] *Key Laboratory of Geographic Information Science (Ministry of Education), East China Normal University, 500 Dongchuan Road, Shanghai 200241, PR China*

*Corresponding author. Email: lilinyi@whu.edu.cn

Integration of Bayesian regulation back-propagation neural network and particle swarm optimization for enhancing sub-pixel mapping of flood inundation in river basins

Sub-pixel mapping of flood inundation (SMFI) is one of hotspots in remote sensing and relevant research and application fields. In this study, a novel method based on the integration of Bayesian regulation back-propagation neural network (BRBP) and particle swarm optimization (PSO), so-called IBRBPPSO, is proposed for SMFI in river basins. The IBRBPPSO-SMFI algorithm was developed and evaluated using Landsat images from the Changjiang River Basin in China and the Murray-Darling Basin in Australia. Compared with traditional SMFI methods, IBRBPPSO-SMFI consistently achieves the most accurate SMFI results in terms of visual and quantitative evaluations. IBRBPPSO-SMFI is superior to PSO-SMFI with not only an improved accuracy, but also an accelerated convergence speed of the algorithm. IBRBPPSO-SMFI reduces the uncertainty in mapping inundation in river basins by improving the accuracy of SMFI. The result of this study will also enrich the SMFI methodology, and thereby benefit the environmental studies of river basins.

Keywords: sub-pixel; floods; particle swarm optimization; Bayesian regulation back-propagation neural network; algorithm integration

1. Introduction

Floods are one of the most common and costly natural hazards in the world. The effects of flood inundation can be local, affecting a community, or very large, impacting entire river basins. Flood inundation has spatio-temporal patterns. Remote

sensing technology has been an effective method to provide valuable information on inundation distributions (Chen et al., 2013; Chen et al., 2014; Chen et al., 2015; Huang et al., 2014b; Huang et al., 2015; Rakwatin et al., 2013). However, high temporal-resolution remote sensing imagery generally does not have high spatial resolution (Huang et al., 2014a; Li et al., 2015b). The accuracy of inundation mapping using high temporal-resolution remote sensing imagery is substantially compromised due to mixed pixels caused by spatial resolution constraints.

Sub-pixel mapping can be applied to improve the accuracy of inundation mapping from high temporal-resolution remote sensing imagery. Sub-pixel mapping is to obtain the spatial distribution information within mixed pixels based on the spatial dependence assumption that observations close together are more alike than those that are further apart (Atkinson, 2005). There have been various methods developed for sub-pixel mapping, such as pixel swapping algorithm (Atkinson, 2005; Huang et al., 2014a), spatial attraction models (SAM; (Mertens et al., 2006)), genetic algorithm (Mertens et al., 2003; Li et al., 2015a), artificial neural networks (Mertens et al., 2004; Zhang et al., 2008), and particle swarm optimization (PSO; (Li et al., 2015b)). However, due to the complexity and uncertainty of remote sensing imagery, sub-pixel mapping of flood inundation (SMFI) is still a difficult task. Therefore, there is a need to improve the mapping accuracy and to reduce the uncertainty of SMFI. SMFI is an optimization issue in essence (Li et al., 2015b). PSO is a relatively new swarm intelligence method which possesses an ability to search for the optimal solutions for optimization issues (Bratton and Kennedy, 2007; Kennedy and Eberhart, 1997) and

has the potential to improve accuracy in mapping inundation at a sub-pixel scale (Li et al., 2015b). Bayesian regulation back-propagation neural network (BRBP) is trained to map the input samples on the correct outputs through back-propagation based on Bayesian regulation. Bayesian regulation minimizes a combination of squared errors and weights, and then determines the correct combination so as to produce a network that is well generalized (The MathWorks, Inc., 2015). The assumption of this study is that the performance of PSO-SMFI should be enhanced if coupled with BRBP-SMFI. The results of BRBP-SMFI can be used as prior knowledge to be integrated into the evolution process of PSO-SMFI for optimal solutions. Compared with standard PSO-SMFI, the integration method is expected not only to improve the accuracy of SMFI, but also to accelerate the convergence speed of the algorithm.

In this study, the above assumption was tested by developing an integration method of BRBP and PSO for SMFI (IBRBPPSO-SMFI) from remote sensing imagery. The main objectives are (1) to build the IBRBPPSO-SMFI algorithm; (2) to compare the effects of IBRBPPSO-SMFI with traditional SMFI methods using Landsat Thematic Mapper/Enhanced Thematic Mapper Plus (TM/ETM+) images of river basins in China and Australia.

2. Methodology

SMFI is used to obtain the sub-pixel spatial distribution of flood inundation within mixed pixels by maximizing their spatial dependence while maintaining the original proportions of inundation within the mixed pixels (Li et al., 2015b). PSO is a relatively new evolutionary computing method which uses a swarm of individuals to

probe the best position in the search space (Bratton and Kennedy, 2007; Kennedy and Eberhart, 1997). Suppose the search space is *M*-dimensional and that there are *N* individuals in the swarm, then the position of the *i*th particle is denoted as X_i with X_i having coordinates $(x_{i1}, x_{i2}, \ldots, x_{iM})$, which represents a possible solution. The value of x_{im} $(1 \le m \le M)$ here is restricted to 0 or 1. The best previous position discovered by the whole swarm represents the best solution of an optimal problem in PSO. The SMFI results of BRBP can be used as prior knowledge to be integrated into the evolution process of the PSO method for optimal solutions. A flow chart for IBRBPPSO-SMFI is shown in Figure 1. The fitness function of IBRBPPSO-SMFI is the same as that of PSO-SMFI (Li et al., 2015b).

INSERT FIGURE 1 HERE

Compared with PSO-SMFI, there are two characteristics in IBRBPPSO-SMFI: the acquisition of BRBP-SMFI results as prior knowledge and the integration of BRBP and PSO for SMFI.

(a) Acquisition of BRBP-SMFI results as prior knowledge

BRBP-SMFI constructs a local SMFI model describing the relationship between inundation fractions in a local region and sub-pixel distributions within the central mixed pixel of the region. Local region consists of 3×3 pixels including a central pixel and its 8 surrounding neighbours. Therefore, there are 8 neurons in the input layer, corresponding to 8 surrounding neighbours. Let S represent the scale factor between a mixed pixel and its sub-pixels. When $S = 5$, there are 25 neurons in the output layer, corresponding to the distributions of 25 sub-pixels within the central

mixed pixel. Compared with standard back-propagation (SBP), BRBP has better convergence performance in the training process, which benefits the SMFI results.

(b) Integration of BRBP and PSO for SMFI

Algorithm integration exchanges vector values between the position of the particle and BRBP-SMFI result to generate a new position. An example of the integration is shown in Figure 2 where inundation is represented by 1 and non-inundation is represented by 0. Each mixed pixel is made up of 5×5 sub-pixels when $S=5$. The vectors in Figure 2 are obtained by placing each sub-pixel row of the corresponding mixed pixels. The exchange point is randomly generated within the integer domain 1 to 25. The integration attaches the first part (in pink) of the position of the particle to the second part (in green) of BRBP-SMFI result to generate a new position. The fitness value of the new position is compared with the fitness value of the previous one. If the fitness value of the new position is higher, then replace the previous position with the new one.

INSERT FIGURE 2 HERE

3. Case study

3.1 Materials

Two comparative study areas from China and Australia were selected for the case study. Landsat TM/ETM+ images were acquired when there were significant flood events in these areas. Key characteristics of the two study areas are summarized in Table 1.

INSERT TABLE 1 HERE

Materials of the two comparative study areas are shown in Figure 3. Locations of the two study areas are shown in color composite (R5G2B1) images in Figures 3(a) and (d), respectively. Figures 3(b) and (e) are reference images which were obtained from the corresponding Landsat images at 30m resolution using the modified normalized difference water index (mNDWI; (Xu, 2006)). In the case study, the scale factor S was set at 5, which was adopted from the value commonly used in sub-pixel mapping from remote sensing images (Ge et al., 2014; Li et al., 2015b). Figures 3(c) and (f) are inundation fraction images which were derived by aggregating the corresponding inundation reference images. The value of the aggregated pixel equals to the proportion of inundation pixels inside the corresponding 5×5 window. Therefore, the resolution of inundation fraction images is 150m. The inundation fraction images were used as the inputs of the SMFI methods for comparisons.

INSERT FIGURE 3 HERE

3.2 Study methods

The five SMFI methods for comparisons in the study are SAM-SMFI, SBP-SMFI, BRBP-SMFI, PSO-SMFI and IBRBPPSO-SMFI. The inputs to these methods were the same flood inundation fraction images. The same surrounding neighbouring type was used for all SMFI methods. Descriptions of different SMFI methods are shown in Table 2.

INSERT TABLE 2 HERE

3.3 Results and discussion

Visual comparisons of the five SMFI methods in the two study areas are shown in Figure 4 and Figure 5, respectively. To ensure clarity in comparing the methods, the same small regions from the reference images and SMFI results are zoomed and shown in Figure 4 and Figure 5, respectively. In Figure 4, BRBP-SMFI performs better than SBP-SMFI. The result of BRBP-SMFI is more similar to the reference image than that of SBP-SMFI in visualization. That is because BRBP has better convergence performance than SBP in the neural network training process, which benefits the SMFI result. IBRBPPSO-SMFI obtains the best SMFI result among the five SMFI methods for the Changjiang River Basin. IBRBPPSO-SMFI maps the Changjiang River and its tributaries more continuously and smoothly than other SMFI methods. From Figure 5, IBRBPPSO-SMFI also obtains the best visual SMFI result among the five SMFI methods for the Murray-Darling Basin.

INSERT FIGURE 4 HERE

INSERT FIGURE 5 HERE

Table 3 shows the quantitative comparisons of the five SMFI methods in the two study areas. We compare the SMFI results using the measures of overall accuracy (OA), Kappa coefficient, average producer's accuracy (APA) and average user's accuracy (AUA) (Foody, 2002). All pure pixels in the flood inundation fraction images are excluded from calculations. From Table 3, we can see that BRBP-SMFI

performs better than SBP-SMFI. Among the five SMFI methods, IBRBPPSO-SMFI exhibits the highest OA, Kappa, APA and AUA in the two study areas. For example, the OA values of SAM-SMFI, SBP-SMFI, BRBP-SMFI, PSO-SMFI and IBRBPPSO-SMFI are 72.4%, 69.6%, 74.2%, 77.7% and 78.8% in Study Area 1, respectively. The OA values of SAM-SMFI, SBP-SMFI, BRBP-SMFI, PSO-SMFI and IBRBPPSO-SMFI are 69.3%, 65.0%, 73.2%, 79.7% and 81.6% in Study Area 2, respectively. The combination of PSO and BRBP can lead to a better performance, because the combination takes advantage of the merits of both PSO and BRBP. The SMFI results of BRBP have been used as prior knowledge to be integrated into the evolution process of the PSO method for optimal solutions.

INSERT TABLE 3 HERE

We further compare PSO-SMFI with IBRBPPSO-SMFI in terms of the convergence performance in Study Area 1 because both are based on PSO which is a stochastic optimization algorithm. The results are shown in Figure 6 where IN represents iterative number. IBRBPPSO-SMFI has better convergence performance in SMFI accuracy and convergence speed than PSO-SMFI. For example, the OA value of PSO-SMFI is 78.8% at the 20th iteration while IBRBPPSO-SMFI obtains this OA value only at the 10th iteration.

INSERT FIGURE 6 HERE

4. Conclusions

In this study, a new integration method called IBRBPPSO-SMFI is proposed to

achieve improved performance in SMFI in river basins. The IBRBPPSO-SMFI algorithm was developed. We assessed the results of IBRBPPSO-SMFI using Landsat TM/ETM+ images from the Changjiang River Basin in China and the Murray-Darling Basin in Australia. IBRBPPSO-SMFI obtains the most accurate SMFI results among the five SMFI methods in terms of visual comparisons and quantitative comparisons in the two river basins. IBRBPPSO-SMFI not only has a higher accuracy of SMFI, but also has a higher convergence speed of the algorithm than PSO-SMFI. Therefore, the assumption that coupled with BRBP, the performance of the PSO method can be enhanced has proved to be valid. IBRBPPSO-SMFI reduces the uncertainty in mapping flood inundation in river basins by improving the accuracy of SMFI. The result of this study will also enrich the SMFI methodology and facilitate the application of high temporal-resolution remote sensing imagery in inundation mapping, and thereby benefit the environmental studies of river basins.

Acknowledgements

This paper was supported by the National Natural Science Foundation of China (Grant No. 41371343 and Grant No. 41001255). The authors also wish to thank their colleague Susan Cuddy for her helpful discussions and constructive suggestions.

References

Atkinson, P.M. 2005. “Sub-pixel Target Mapping from Soft-classified, Remotely Sensed Imagery.” *Photogrammetric Engineering and Remote Sensing* 71: 839-846.

Bratton, D., and Kennedy, J. 2007. “Defining a Standard for Particle Swarm Optimization.” In *IEEE Swarm Intelligence Symposium*, Hawaii, USA.

Chen, Y., Huang, C., Ticehurst, C., Merrin, L., and Thew, P. 2013. “An Evaluation of MODIS Daily and 8-day Composite Products for Floodplain and Wetland Inundation Mapping.” *Wetlands* 33: 823-835. doi: 10.1007/s13157-013-0439-4.

Chen, Y., Liu, R., Barrett, D., Gao, L., Zhou, M., Renzullo, L. and Emelyanova, I. 2015. “A Spatial Assessment Framework for Evaluating Flood Risk under Extreme Climates.” *Science of the Total Environment* 538: 512-523. doi: 10.1016/j.scitotenv.2015.08.094.

Chen, Y., Wang, B., Pollino, C., Cuddy, S., Merrin, L., and Huang, C. 2014. “Estimate of Flood Inundation and Retention on Wetlands using Remote Sensing and GIS.” *Ecohydrology* 7: 1412-1420. doi: 10.1002/eco.1467.

Foody, G.M. 2002. “Status of Land Cover Classification Accuracy Assessment.” *Remote Sensing of Environment* 80: 185-201. doi: 10.1016/S0034-4257(01)00295-4.

Ge, Y., Chen, Y., Li, S., and Jiang Y. 2014. “Vectorial Boundary-Based Sub-Pixel Mapping Method for Remote-Sensing Imagery.” *International Journal of Remote Sensing* 35: 1756-1768. doi: 10.1080/01431161.2014.882034.

Huang, C., Chen, Y., and Wu, J. 2014a. “DEM-based Modification of Pixel-swapping Algorithm for Enhancing Floodplain Inundation Mapping.” *International Journal of Remote Sensing* 35: 365-381. doi: 10.1080/01431161.2013.871084.

Huang, C., Chen, Y., and Wu, J. 2014b. “Mapping Spatio-temporal Flood Inundation Dynamics at Large River Basin Scale using Time-series Flow Data and MODIS Imagery.” *International Journal of Applied Earth Observation and Geoinformation* 26: 350-362. doi: 10.1016/j.jag.2013.09.002.

Huang, C., Chen, Y., Wu, J., Li, L., and Liu R. 2015. “An Evaluation of Suomi NPP-VIIRS Data for Surface Water Detection.” *Remote Sensing Letters* 6: 155-164. doi: 10.1080/2150704X.2015.1017664.

Kennedy, J. and Eberhart, R. 1997. “A Discrete Binary Version of the Particle Swarm Algorithm.” In *IEEE International Conference on Systems, Man, and Cybernetics*, Piscataway, USA.

Li, L., Chen, Y., Xu, T., Liu R., Shi, K., and Huang, C. 2015a. “Super-resolution Mapping of Wetland Inundation from Remote Sensing Imagery Based on Integration of Back-propagation Neural Network and Genetic Algorithm.” *Remote Sensing of Environment* 164: 142-154. doi: 10.1016/j.rse.2015.04.009.

Li, L., Chen, Y., Yu, X., Liu R., and Huang, C. 2015b. “Sub-Pixel Flood Inundation Mapping from Multispectral Remotely Sensed Images Based on Discrete Particle Swarm Optimization.” *ISPRS Journal of Photogrammetry and Remote Sensing* 101: 10-21. doi: 10.1016/j.isprsjprs.2014.11.006.

Mertens, K.C., De Baets, B., Verbeke, L.P.C., and De Wulf, R. R. 2006. “A Sub-pixel Mapping Algorithm Based on Sub-pixel/pixel Spatial Attraction Models.” *International Journal of Remote Sensing* 27: 3293-3310. doi: 10.1080/01431160500497127.

Mertens, K.C., Verbeke, L.P.C., Ducheyne, E.I., and De Wulf, R. R. 2003. “Using Genetic Algorithms in Sub-pixel Mapping.” *International Journal of Remote Sensing* 24: 4241-4247. doi: 10.1080/0143116031000159507 3.

Mertens, K.C., Verbeke, L.P.C., Westra, T., and De Wulf, R. R. 2004. “Sub-pixel Mapping and Sub-pixel Sharpening using Neural Network Predicted Wavelet Coefficients.” *Remote Sensing of Environment* 91: 225-236. doi: 10.1016/j.rse.2004.03.003.

Rakwatin, P., Sansena, T., Marjang, N., and Rungsipanich, A. 2013. "Using Multi-temporal Remote-sensing Data to Estimate 2011 Flood Area and Volume over Chao Phraya River Basin, Thailand." *Remote Sensing Letters* 4: 243-250. doi: 10.1080/2150704X.2012.723833.

The MathWorks, Inc. 2015. Neural Network Toolbox Documentation. http://cn.mathworks.com/help/nnet/ref/trainbr.html?searchHighlight=trainbr.

Xu, H. 2006. "Modification of Normalised Difference Water Index (NDWI) to Enhance Open Water Features in Remotely Sensed Imagery." *International Journal of Remote Sensing* 27: 3025-3033.

Zhang, L., Wu, K., Zhong, Y., and Li, P. 2008. "A new Sub-pixel Mapping Algorithm Based on a BP Neural Network with an Observation Model." *Neurocomputing* 71: 2046-2054. doi: 10.1016/j.neucom.2007.08.033.

Table 1. Key characteristics of the two study areas.

	Study Area 1	Study Area 2
Location	Changjiang River Basin of China	Murray-Darling Basin of Australia
Area (km^2)	225	3600
Data	Landsat 7 ETM+ imagery	Landsat 5 TM imagery
Date	9 August 2010	2 January 2011
Image size (pixels)	500×500	2000×2000
Image resolution (m)	30	30

Table 2. Descriptions of different SMFI methods.

Method	Parameter description	Parameter value
SAM	none	none
SBP	number of hidden layers	1
	learning rate	0.01
BRBP	number of hidden layers	1
	Marquardt adjustment parameter (MAP)	0.005
	decrease factor for MAP	0.1
	increase factor for MAP	10

PSO	maximum inertia weight	0.9
	minimum inertia weight	0.4
	size of the swarm	10
	maximum iterative number	10
IBRBPPSO	maximum inertia weight	0.9
	minimum inertia weight	0.4
	size of the swarm	10
	maximum iterative number	10

Table 3. Quantitative comparisons of different SMFI methods.

Method	Study Area 1				Study Area 2			
	OA (%)	Kappa coefficient	APA (%)	AUA (%)	OA (%)	Kappa coefficient	APA (%)	AUA (%)
SAM	72.4	0.397	69.0	71.7	69.3	0.374	68.4	69.9
SBP	69.6	0.346	66.8	68.1	65.0	0.293	64.6	64.8
BRBP	74.2	0.445	71.7	73.3	73.2	0.459	72.9	73.0
PSO	77.7	0.533	76.7	76.7	79.7	0.593	79.6	79.6
IBRBPPSO	78.8	0.556	77.8	77.8	81.6	0.630	81.5	81.5

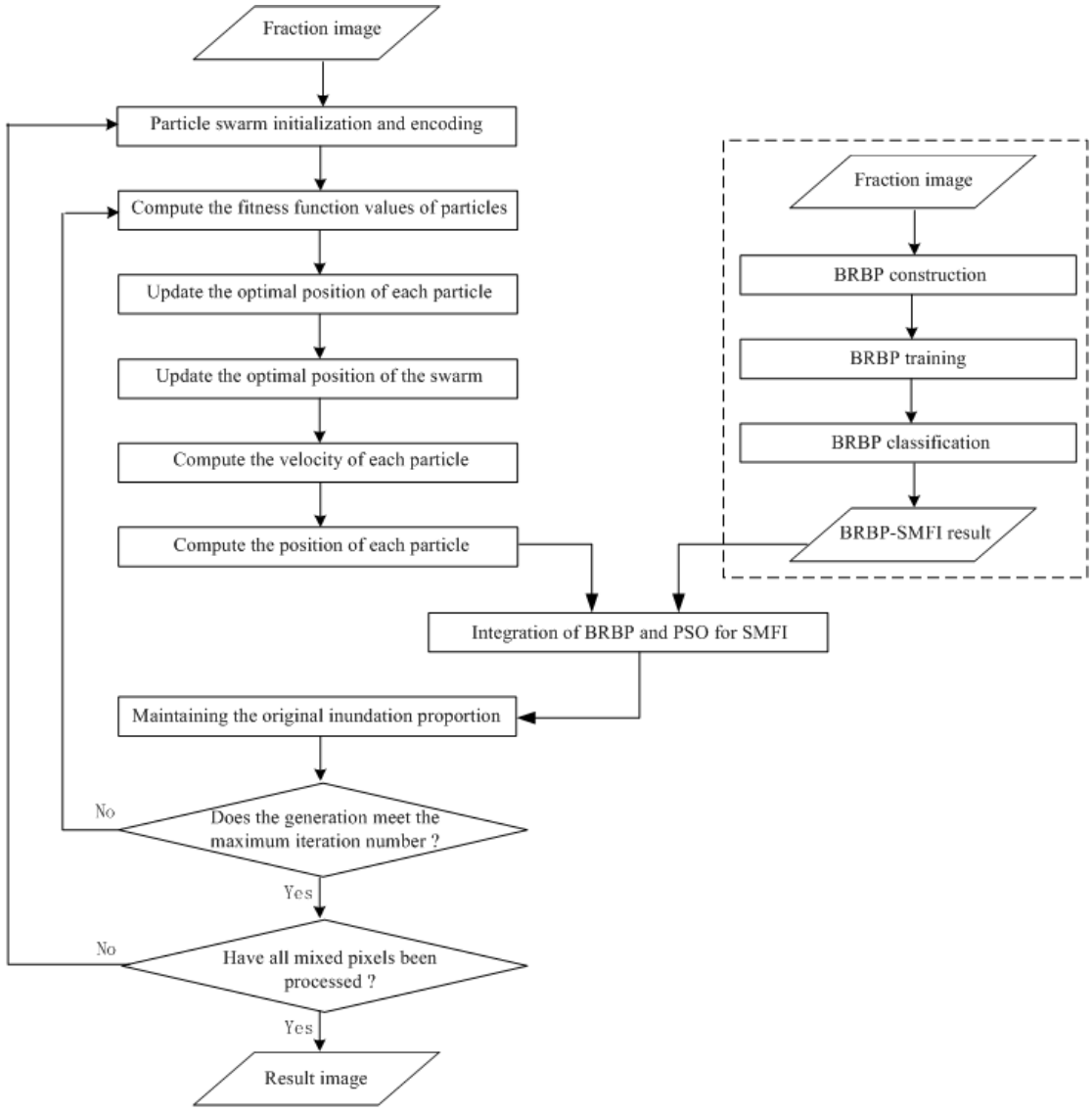

Figure 1. Flow chart for IBRBPPSO-SMFI.

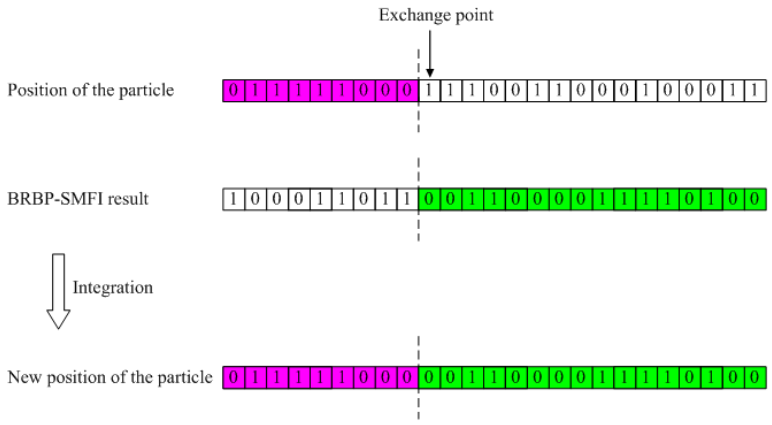

Figure 2. An example of algorithm integration (S=5).

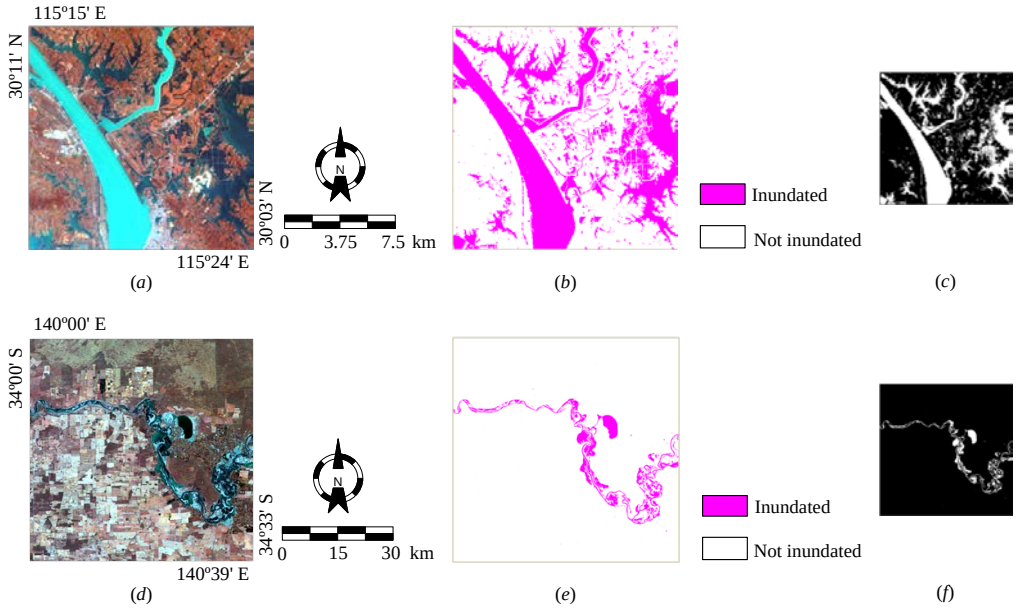

Figure 3. Materials of the two comparative study areas (S=5). (*a*) Location of Study Area 1 shown in a color composite (R5G2B1) Landsat 7 ETM+ image (500×500 pixels) at 30m resolution after image enhancement. (*b*) Inundation reference image (500×500 pixels) at 30m resolution. (*c*) Inundation fraction image (100×100 pixels) at 150m resolution. (*d*) Location of Study Area 2 shown in a color composite (R5G2B1) Landsat 5 TM image (2000×2000 pixels) at 30m resolution after image enhancement. (*e*) Inundation reference image (2000×2000 pixels) at 30m resolution. (*f*) Inundation fraction image (400×400 pixels) at 150m resolution.

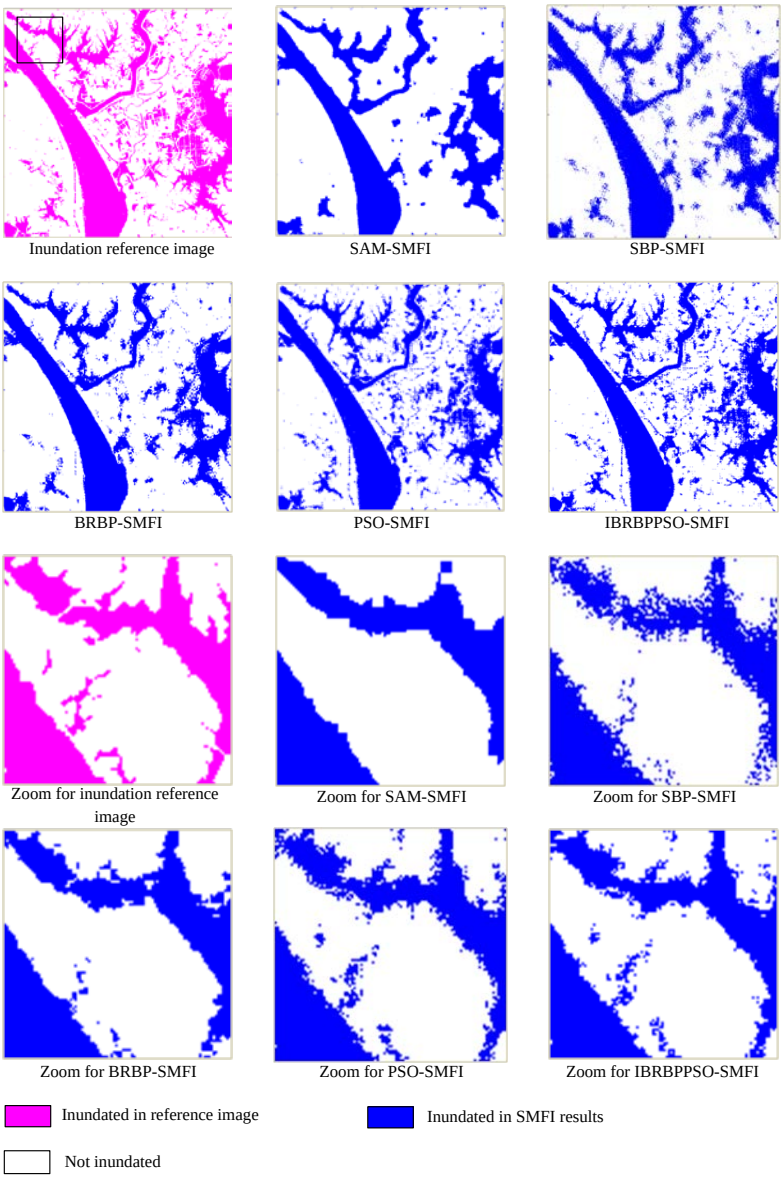

Figure 4. Visual comparisons of the five SMFI methods in Study Area 1 (500×500 pixels, *S*=5).

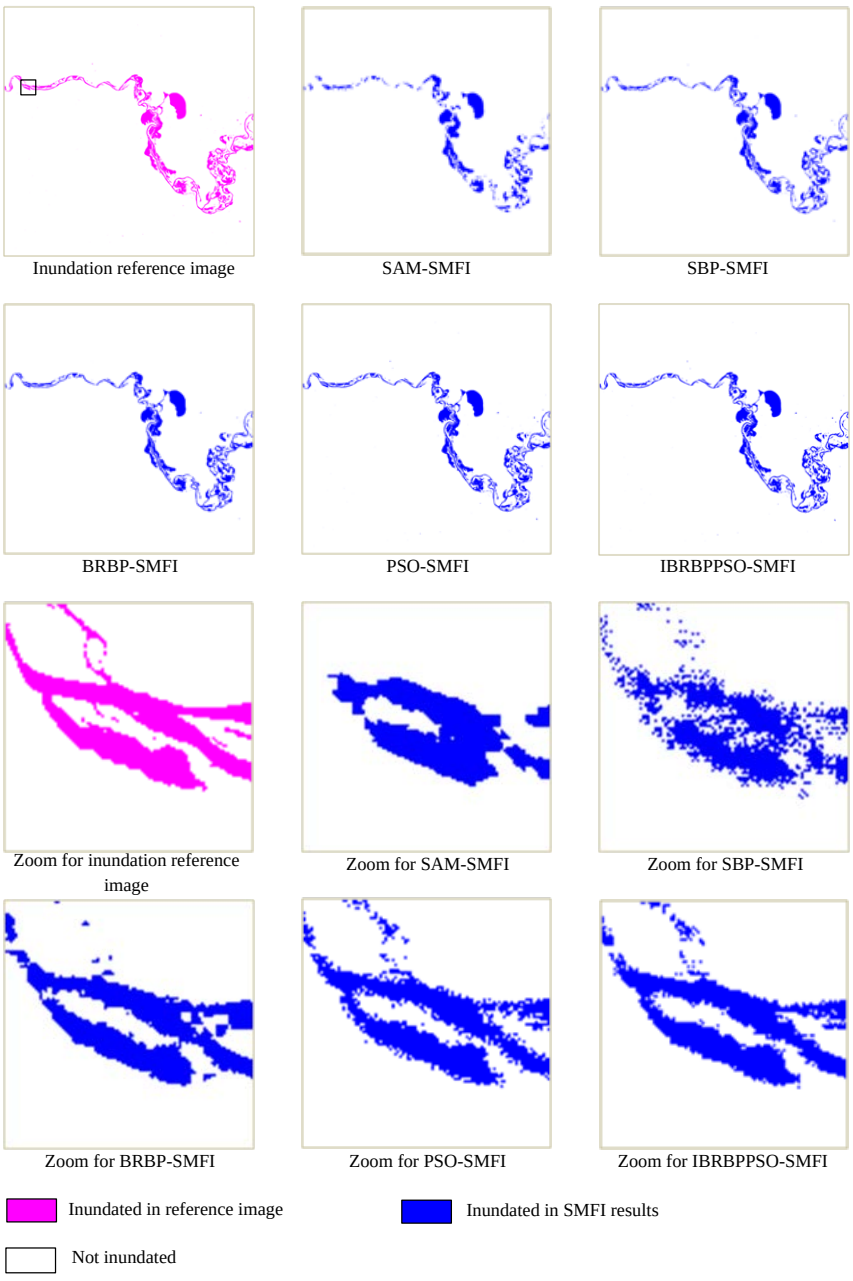

Figure 5. Visual comparisons of the five SMFI methods in Study Area 2 (2000×2000 pixels, *S*=5).

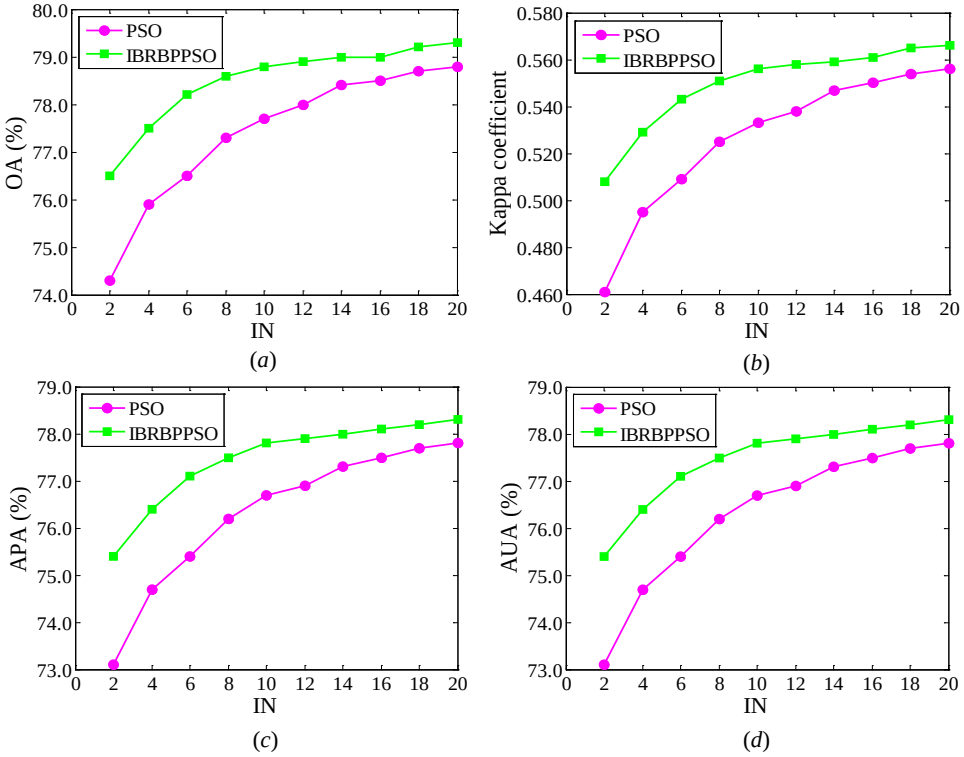

Figure 6. Convergence performance of PSO-SMFI and IBRBPPSO-SMFI in Study Area 1. (*a*) Convergence performance of OA. (*b*) Convergence performance of Kappa coefficient. (*c*) Convergence performance of APA. (*d*) Convergence performance of AUA.